HIGH TECHNOLOGY LETTERS | Vol. 29 No. 3 | Sep. 2023 | pp. 247-256

doi:10.3772/j.issn.1006-6748.2023.03.003

Research and experimental analysis of precision degradation method based on the ball screw mechanism①

KONG Deshun(孔德顺)[*,**], GAO Xiangsheng[***,****], JIANG Huizeng②[*,**]

([*] Institute of Standard Metrology, China Academy of Railway Sciences Corporation Limited, Beijing 100081, P. R. China)
([**] Beijing Huaheng Technology Co. Ltd., Beijing 100081, P. R. China)
([***] Key Laboratory of Advanced Manufacturing Technology, Beijing University of Technology, Beijing 100124, P. R. China)
([****] Hebei Changxiang Rubber Plastic Technology Co. Ltd., Hengshui 053500, P. R. China)

Abstract

As a key transmission component in computer numerical control (CNC) machine tools, the ball screw mechanism (BSM) is usually investigated under working load conditions. Its accuracy degradation process is relatively long, which is not conducive to the design and development of new products. In this paper, the normal wear depth of the BSM nut raceway is calculated under the variable speed operation condition using the fractal wear analysis method and the BSM's accelerated degradation proportional wear model. Parameters of the acceleration degradation model of the double-nut preloaded ball screw pair are calculated based on the physical simulation results. The accelerated degradation test platform of the BSM is designed and manufactured to calculate the raceway wear model when the lubrication condition is broken under the variable-speed inertial load and the boundary lubrication condition under the uniform speed state. Three load forces and two samples are selected for the accelerated degradation test of the BSM. The measured friction torque of the BSM is employed as the evaluation index of the accuracy degradation test. In addition, the life cycle of the accuracy retention is accurately calculated by employing the parameters of the physical simulation model of the BSM. The calculations mentioned above can be used to estimate BSM's accuracy performance degradation law under normal operating conditions. The application of the proposed model provides a new research method for researching the precision retention of the BSM.

Key words: ball screw mechanism (BSM), fractal theory, wear model, accelerated degradation method, friction torque, precision retention

0 Introduction

As a key part of the numerical control machine tool, the precision degradation process of the ball screw mechanism (BSM) under a normal working load is relatively long, which is not conducive to the design and development of new products. Most researchers use experimental methods to shorten the test cycle of precision degradation of BSM and explore BSM's failure mode or accuracy variation characteristics. The surface pitting corrosion, structural failure mode, and fatigue life of the BSM were experimentally studied by Shimoda et al.[1]. Zhang et al.[2] explored the fast wear of the screw raceway based on the wear situation of the screw raceway and nut raceway by combining the mathematical modeling of lubrication and elastic contact stress. Fleischer et al.[3] used the adaptive lubrication method to improve BSM wear. Zhen and An[4] analyzed the influence law of ball dimensional tolerance, axial load, radial load, and dimensional ball accuracy on the service life of the BSM. Li et al.[5] proposed a systematic method of BSM prediction that can achieve fault diagnosis, early diagnosis, health assessment, and life prediction. Deng et al.[6] proposed the hybrid gated recurrent unit-particle filter (GRU-PF) method to achieve the life prediction of the BSM. These investigations are only qualitative research on the precision degradation characteristics of ball screw.

According to the structural parameters, perform-

① Supported by the National Natural Science Foundation of China (No. 51575014, 51505020) and the Key Foundation Project of China Academy of Railway Sciences (No. 2021YJ200).
② To whom correspondence should be addressed. E-mail: 15053100756@163.com.
Received on Nov. 18, 2022

ance degradation characteristics, and working conditions of the BSM, the performance evaluation of BSM was achieved by combining qualitative analysis and quantitative calculation [7-8]. Shen [9] proposed a precision degradation model of BSM based on the contact deformation and motion law between the ball and the raceway of a double-nut preloaded BSM. Moreover, the author combined the model with the adhesive wear law and the quantitative relationship between working conditions, structural parameters, and precision degradation of the BSM. Chen et al. [10] analyzed the contact stress and the roller-slip relationship between the ball and the raceway. The test verified that the speed and the load greatly affect the relationship mentioned above. It was found that friction and wear were the main reasons for the precision decline of BSM. Zhou et al. [11] established the load distribution and velocity change models that can accurately predict the performance and life of the double-nut BSM. Liu et al. [12] used fractal geometry theory to analyze the microscopic morphology representation of raceway and ball surfaces. The authors combined the microscopic morphology representation of threaded groove surface and a multi-scale contact mechanics model. Lastly, the authors determined that the accuracy degree decline increased with the axial load and rotational speed. Zhao et al. [13] established a wear model to analyze the change law of wear depth. Moreover, the author combined the proposed model with Archard theory and the iterative interpolation algorithm and investigated the precision life degradation law of a double-nut ball screw. Similarly, Zhang et al. [14] proposed a BSM degradation model by using the wear amount, load, stroke, and experimental data. These investigations are based on detailed theoretical models to quantitatively study the precision life degradation mechanism of BSM, but it is difficult to accurately predict the precision degradation law of BSM.

The preload and friction torque are typically used as the evaluation indexes of the BSM's precision degradation. BSM wear will reduce the preload and friction torque. Firstly, the parameters of the accelerated degradation model are estimated via the maximum likelihood estimation method using the fractal adhesive contact wear model. The Weibull distribution function of accuracy evaluation under different stress levels was ensured to be consistent by employing the proportional wear model of the accelerated degradation of BSM[15-16]. Secondly, the calculation method of raceway wear depth under ball screw transmission conditions is considered. Finally, the accelerated degradation method of the BSM is verified by using the accelerated degradation BSM test bench, providing a new method for the research on BSM accuracy retention.

1 BSM wear model

An increase in the truncation between the ball and the rough fractal surface profile of the raceway will increase the material removal caused by the contact of the fully plastic micro convex body. If the interference increment d_h is set as the minimum local interference δ_{min} [17] and the circular contact wear particles are generated by the contact of all fully plastic micro convex bodies, then

$$d_h = \delta_{min} = 2G^{(D_s-2)} (\ln\gamma)^{1/2} (2r_s')^{(3-D_s)} \tag{1}$$

$$dV_{p1} = \left(\frac{a' - \pi\delta^2}{2} + \pi R\delta\right)d_h - \pi(R-\delta)d_h^2 - \frac{\pi}{3}d_h^3 \tag{2}$$

where, r_s' is the truncation radius of the minimum micro-convex body contact, R is the radius of the sphere of the removed table, a' is the area of the larger bottom surface, d_h is the height from the larger to the smaller bottom surface, and δ is the distance from the larger bottom surface of the table to the top of the entire ball. Therefore, the wear volume of a single micro-convex body can be approximated by the volume of the table as follows.

Substituting $\delta = 2G^{(D_s-2)} (\ln\gamma)^{1/2} (2r')^{(3-D_s)}$ yields: $R = \frac{(a')^{(D_s-1)/2}}{2^{(5-D_s)}\pi^{(D_s-1)/2}G^{(D_s-2)}(\ln\gamma)^{1/2}}$, $a' = \pi(r')^2$, while Eq. (1) can be substituted into Eq. (2) and simplified to obtain:

$$dV_{p1} = a'd_h - 2\pi\left(\frac{4}{\pi}\right)^{(3-D_s)} d_h G^{2(D_s-2)} \ln\gamma a'^{(3-D_s)} - \frac{\pi d_h^2 a'^{(D_s-1)/2}}{2^{(5-D_s)}\pi^{(D_s-1)/2}G^{(D_s-2)}(\ln\gamma)^{1/2}} + 2\pi d_h^2 G^{(D_s-2)} (\ln\gamma)^{1/2} \left(\frac{4a'}{\pi}\right)^{(3-D_s)/2} - \frac{\pi}{3}d_h^3 \tag{3}$$

Without considering the influence of time, the wear amount of single contact on the entire contact surface can be calculated by integrating the following expression:

$$dV_p = \int_{a_s'}^{a_c'} dV_{p1}(a')n(a', a_L')\,da' \tag{4}$$

Equation $n(a') = -\frac{dN(a')}{da'} = \frac{(D_s-1)}{2a_L'}\left(\frac{a_L'}{a'}\right)^{(D_s+1)/2}$ and Eq. (3) are substituted into Eq. (4), and integral calculation results are obtained as

$$dV_{\mathrm{p}} = \frac{(D_{\mathrm{s}}-1)}{2}{a_{\mathrm{L}}}'^{(D_{\mathrm{s}}-1)/2}d_{\mathrm{h}}\left[\frac{2}{(3-D_{\mathrm{s}})}a'^{(3-D_{\mathrm{s}})/2} - \frac{4\pi\ln\gamma}{(7-3D_{\mathrm{s}})}\left(\frac{4}{\pi}\right)^{(3-D_{\mathrm{s}})}G^{2(D_{\mathrm{s}}-2)}a'^{(7-3D_{\mathrm{s}})/2} - \frac{\pi d_{\mathrm{h}}\ln a'}{2^{(5-D_{\mathrm{s}})}\pi^{(D_{\mathrm{s}}-1)/2}G^{(D_{\mathrm{s}}-2)}(\ln\gamma)^{1/2}} + \frac{2\pi d_{\mathrm{h}}}{(2-D_{\mathrm{s}})}G^{(D_{\mathrm{s}}-2)}(\ln\gamma)^{1/2}\left(\frac{4}{\pi}\right)^{(3-D_{\mathrm{s}})/2}a'^{(2-D_{\mathrm{s}})} - \frac{2\pi d_{\mathrm{h}}^{2}}{3(1-D_{\mathrm{s}})}a'^{(1-D_{\mathrm{s}})/2}\right]_{a_{\mathrm{s}}'}^{a_{\mathrm{c}}'},\ D_{\mathrm{s}} \neq \frac{7}{3} \tag{5}$$

and

$$dV_{\mathrm{p}} = \frac{(D_{\mathrm{s}}-1)}{2}{a_{\mathrm{L}}}'^{(D_{\mathrm{s}}-1)/2}d_{\mathrm{h}}\left[\frac{2}{(3-D_{\mathrm{s}})}a'^{1/3} - 2\pi\left(\frac{4}{\pi}\right)^{(3-D_{\mathrm{s}})}G^{2(D_{\mathrm{s}}-2)}\ln\gamma\ln a' - \frac{\pi d_{\mathrm{h}}\ln a'}{2^{(5-D_{\mathrm{s}})}\pi^{(D_{\mathrm{s}}-1)/2}G^{(D_{\mathrm{s}}-2)}(\ln\gamma)^{1/2}} + \frac{2\pi d_{\mathrm{h}}}{(2-D_{\mathrm{s}})}G^{(D_{\mathrm{s}}-2)}(\ln\gamma)^{1/2}\left(\frac{4}{\pi}\right)^{(3-D_{\mathrm{s}})/2}a'^{-1/3} - \frac{2\pi d_{\mathrm{h}}^{2}}{3^{(1-D_{\mathrm{s}})}}a'^{-2/3}\right]_{a_{\mathrm{s}}'}^{a_{\mathrm{c}}'},\ D_{\mathrm{s}} = \frac{7}{3} \tag{6}$$

The raceway contact area wear is calculated by the semi-analytical method by considering the relative sliding of the ball and the raceway contact area meshing. It is assumed that the relative sliding velocity of the contact surface is v_{s}, and the normal interference of the maximum micro convex body to be worn off is δ_{c}. According to Ref. [18], the number of the same micro bumps being worn off per unit of time (i. e., the wear frequency of micro bumps) can be expressed as follows.

$$\frac{\mathrm{d}n_{\mathrm{w}}}{\mathrm{d}t} = \frac{v_{\mathrm{s}}}{\delta_{\mathrm{c}}} \tag{7}$$

where $\delta_{\mathrm{c}} = 2G^{(D_{\mathrm{s}}-2)}(\ln\gamma)^{1/2}(2\sqrt{2}r_{\mathrm{c}}')^{(3-D_{\mathrm{s}})}$.

The wear volume of a single micro convex body per unit of time can be written as

$$\frac{\partial(dV_{\mathrm{p1}})}{\partial t} = \frac{\mathrm{d}n_{\mathrm{w}}}{\mathrm{d}t}dV_{\mathrm{p1}} = \frac{v_{\mathrm{s}}}{\delta_{\mathrm{c}}}dV_{\mathrm{p1}} \tag{8}$$

According to the equation $n(a') = -\frac{\mathrm{d}N(a')}{\mathrm{d}a'} = \frac{(D_{\mathrm{s}}-1)}{2a_{\mathrm{L}}'}\left(\frac{a_{\mathrm{L}}'}{a'}\right)^{(D_{\mathrm{s}}+1)/2}$ and Eqs (7) and (8), the wear velocity per unit time of the entire equivalent contact surface can be written as

$$\frac{\partial(dV_{\mathrm{p}})}{\partial t} = \int_{a_{\mathrm{s}}'}^{a_{\mathrm{c}}'}\frac{v_{\mathrm{s}}}{\delta_{\mathrm{c}}}dV_{\mathrm{p1}}(a')n(a',{a_{\mathrm{L}}}')\mathrm{d}a' \tag{9}$$

Equation $n(a') = -\frac{\mathrm{d}N(a')}{\mathrm{d}a'} = \frac{(D_{\mathrm{s}}-1)}{2a_{\mathrm{L}}'}\left(\frac{a_{\mathrm{L}}'}{a'}\right)^{(D_{\mathrm{s}}+1)/2}$ and Eq. (3) are substituted into Eq. (9) to obtain integral calculation results:

$$\frac{\partial(dV_{\mathrm{p}})}{\partial t} = \frac{v_{\mathrm{s}}}{\delta_{\mathrm{c}}}dV_{\mathrm{p}} = \frac{v_{\mathrm{s}}}{\delta_{\mathrm{c}}}\frac{(D_{\mathrm{s}}-1)}{2}{a_{\mathrm{L}}}'^{(D_{\mathrm{s}}-1)/2}d_{\mathrm{h}}\left[\frac{2}{(3-D_{\mathrm{s}})}a'^{(3-D_{\mathrm{s}})/2} - \frac{4\pi\ln\gamma}{(7-3D_{\mathrm{s}})}\left(\frac{4}{\pi}\right)^{(3-D_{\mathrm{s}})}G^{2(D_{\mathrm{s}}-2)}a'^{(7-3D_{\mathrm{s}})/2} - \frac{\pi d_{\mathrm{h}}\ln a'}{2^{(5-D_{\mathrm{s}})}\pi^{(D_{\mathrm{s}}-1)/2}G^{(D_{\mathrm{s}}-2)}(\ln\gamma)^{1/2}} + \frac{2\pi d_{\mathrm{h}}}{(2-D_{\mathrm{s}})}G^{(D_{\mathrm{s}}-2)}(\ln\gamma)^{1/2}\left(\frac{4}{\pi}\right)^{(3-D_{\mathrm{s}})/2}a'^{(2-D_{\mathrm{s}})} - \frac{2\pi d_{\mathrm{h}}^{2}}{3(1-D_{\mathrm{s}})}a'^{(1-D_{\mathrm{s}})/2}\right]_{a_{\mathrm{s}}'}^{a_{\mathrm{c}}'},\ D_{\mathrm{s}} \neq \frac{7}{3} \tag{10}$$

and

$$\frac{\partial(dV_{\mathrm{p}})}{\partial t} = \frac{v_{\mathrm{s}}}{\delta_{\mathrm{c}}}dV_{\mathrm{p}} = \frac{v_{\mathrm{s}}}{\delta_{\mathrm{c}}}\frac{(D_{\mathrm{s}}-1)}{2}{a_{\mathrm{L}}}'^{(D_{\mathrm{s}}-1)/2}d_{\mathrm{h}}\left[\frac{2}{(3-D_{\mathrm{s}})}a'^{1/3} - 2\pi\left(\frac{4}{\pi}\right)^{(3-D_{\mathrm{s}})}G^{2(D_{\mathrm{s}}-2)}\ln\gamma\ln a' + \frac{2\pi d_{\mathrm{h}}}{(2-D_{\mathrm{s}})}G^{(D_{\mathrm{s}}-2)}(\ln\gamma)^{1/2}\left(\frac{4}{\pi}\right)^{(3-D_{\mathrm{s}})/2}a'^{-1/3} - \frac{2\pi d_{\mathrm{h}}^{2}}{3(1-D_{\mathrm{s}})}a'^{-2/3} - \frac{\pi d_{\mathrm{h}}\ln a'}{2^{(5-D_{\mathrm{s}})}\pi^{(D_{\mathrm{s}}-1)/2}G^{(D_{\mathrm{s}}-2)}(\ln\gamma)^{1/2}}\right]_{a_{\mathrm{s}}'}^{a_{\mathrm{c}}'},\ D_{\mathrm{s}} = \frac{7}{3} \tag{11}$$

Therefore, the wear rate per unit area and per unit time can be expressed as

$$V_{\mathrm{wat}} = \frac{\partial(dV_{\mathrm{p}})}{\partial t}/L^{2} \tag{12}$$

The motion between the ball and the raceway is compound motion characterized by five motion modes on the macro level [19]. There are three relative angular velocity components $(\omega_x, \omega_y, \omega_z)$ and two relative linear velocity components (v_x, v_y). The angular velocity between the ball and the raceway is ω_x and ω_y. The relative sliding linear velocity component between the ball

and the raceway is denoted as (v_x, v_y), and the angular velocity relative to the spin is denoted as ω_z. Therefore, the relative sliding velocity of any point in the contact area can be expressed as

$$v_s(i,j) = \begin{bmatrix} v_x \\ v_y \end{bmatrix} + \begin{bmatrix} -y(i,j) \\ x(i,j) \end{bmatrix} \omega_z \tag{13}$$

According to the relative motion velocity between the ball and the raceway, the relative motion velocity value in Eq. (13) can be written as $|v_s(i,j)|$. By substituting $|v_s(i,j)|$ into Eqs (10) and (12), the wear rate of any point in the grid cell $V_{wat}(i,j)$ can be obtained. Then, the wear velocity value of a unit point on the grid can be expressed as

$$V_{wt}(i,j) = d_s V_{wat}(i,j) \tag{14}$$

where d_s is the grid cell area.

The wear velocity on different arc sections in the raceway can be expressed as

$$V_{wt}(j) = \sum_{i=1}^{m} V_{wt}(i,j), \ (i,j) \in A_c \tag{15}$$

The wear depth value on the raceway section can be expressed as

$$h_w(j) = \frac{n_b V_{wt}(j) t}{S_s(j)\, dy}, \ (i,j) \in A_c \tag{16}$$

where n_b is the number of the working ball, t is the running time, $S_s(j)$ is the linear length of the raceway, and dy is the grid spacing in the circular direction of the raceway section.

2 Stress analysis of oil film contact

The boundary lubrication state exists between the ball and the raceway during BSM operation, and the oil film and micro-convex body jointly affect the normal load in the contact area. The lubricating oil below the mean height h_m of the fractal surface does not flow, and the lubricating oil above the mean height h_m of the fractal surface is in the elastic fluid state. The discretized oil film thickness distribution in the contact area between the ball and the raceway can be expressed according to the isothermal point contact elastohydrodynamic lubrication theory [20].

$$h_t(i,j) = h_c + \frac{x_i^2}{2R_X} + \frac{y_j^2}{2R_Y} + \delta(x_i, y_j) - \delta(0,0), \ (i,j) \in A_c \tag{17}$$

where, h_c is the oil film thickness at the center of the contact area; R_X and R_Y are the equivalent contact radii of curvature, and $\frac{1}{R_X} = \frac{1}{r_b} - \frac{1}{r_S}$, $\frac{1}{R_Y} = \frac{1}{r_b} + \frac{1}{r_{st}}$.

Moreover, the normal elastic deformation of any point on the grid node in the contact region can be expressed as

$$\delta(x_i, y_j) = \frac{2}{\pi E^*} \iint_{(\xi,\zeta) \in A_c} \frac{P(\xi,\zeta)}{\sqrt{(x_i - \xi)^2 + (y_j \zeta)^2}} \mathrm{d}\xi \mathrm{d}\zeta \tag{18}$$

where $P(\xi,\zeta)$ is the normal stress value in the contact area [21].

The oil film thickness in the center of the contact area can be written as

$$\frac{h_c}{R_e} = H_c^* U_e^{0.68} G_e^{0.49} W_e^{-0.073} \tag{19}$$

$$H_c^* = H_x^* \sin^2\varphi + H_y^* \cos^2\varphi \tag{20}$$

where, φ represents the relative sliding velocity direction of the contact center [17]; U_e, W_e and G_e represent velocity, load, and material parameters, respectively. The parameters mentioned above can be calculated via Eqs (21) and (22).

$$U_e = \frac{\eta_0 u_e}{2E^* R_e}, \ W_e = \frac{Q_{ym}}{2E^* R_e^2}, \ G_e = 2\bar{\alpha} E^* \tag{21}$$

$$\frac{1}{R_e} = \frac{\sin^2\varphi}{R_X} + \frac{\cos^2\varphi}{R_Y}, \ \frac{1}{R_s} = \frac{\cos^2\varphi}{R_X} + \frac{\sin^2\varphi}{R_Y} \tag{22}$$

where η_0 is the dynamic viscosity value of the lubricating oil, u_e is the coiling speed of the lubricating oil, $\bar{\alpha}$ is the viscosity coefficient of the lubricating oil. Then,

$$H_x^* = 4.31 \left\{ 1 - \exp\left[-1.23 \left(\frac{R_Y}{R_X} \right)^{2/3} \right] \right\}$$

$$H_y^* = 4.31 \left\{ 1 - \exp\left[-1.23 \left(\frac{R_X}{R_Y} \right)^{2/3} \right] \right\} \tag{23}$$

The distribution value of oil film thickness in the contact area between the ball and the screw raceway under load can be obtained via Eqs (17) – (23). The total normal load Q_A between the ball and the lead screw raceway is shared by the oil film load Q_{ym} and the micro-convex Q_{wt}. Then,

$$Q_A = Q_{ym} + Q_{wt} \tag{24}$$

3 BSM wear analysis

The motion forms of the ball screw can be divided into accelerated, uniform, and deceleration. The force of the contact point between the ball and the raceway is unbalanced during the acceleration and deceleration of the ball screw, and the lubrication is insufficient, intensifying the wear of the ball and the raceway. The raceway wear depth calculated according to Eq. (16) when the lead screw runs for 1 h under dry friction is shown in Fig. 1. The raceway wear depth when the lead screw runs for 1 h under oil film lubrication is shown in

Fig. 2. According to Fig. 1, when the contact between the ball and the raceway is characterized as dry friction, the wear depth significantly increases with the screw rotation speed. According to Fig. 2, the nut wear depth increases with the screw speed. However, the nut raceway wear depth decreases when the screw speed increases. The main reason for this phenomenon is that the centrifugal force effect increases the oil film thickness, and the oil film jointly bears the normal load of the raceway. Hence, nut raceway wear is reduced due to the sufficient lubrication between the ball and the raceway. Moreover, the analysis of Figs 1 and 2 shows that the raceway wear's contact surface is narrow during film contact lubrication and wider during dry friction contact. The phenomena above can be attributed to the reduction of contact friction and wear between the ball and the raceway due to the oil film.

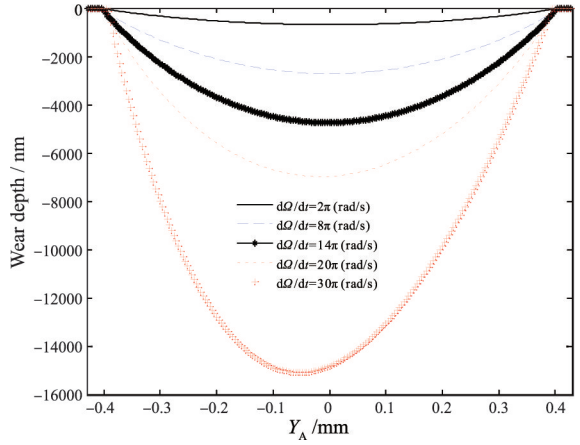

Fig. 1 Distribution of the wear depth along the normal cross-section of the raceway in the same stroke(1 h)

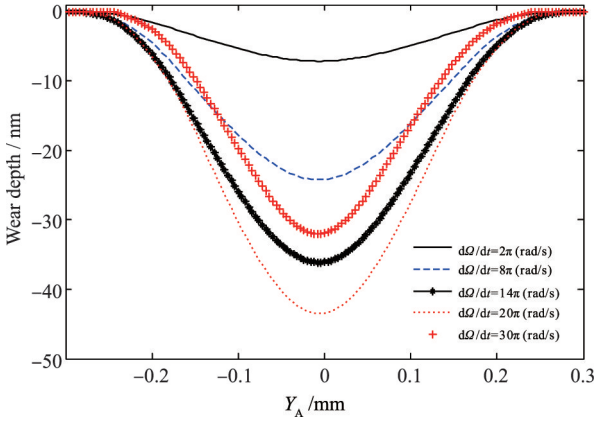

Fig. 2 Distribution of the wear depth along the normal cross-section of the raceway under lubrication condition in the same stroke(1 h)

The test bench for the ball screw pair was designed and processed to investigate the accuracy degradation law of the acceleration test for the ball screw pair, as shown in Fig. 3. Moreover, the accuracy degradation law of the ball screw pair was explored under the following three working conditions.

(1) Uniform rotation (800 r/min) during the entire motion of the lead screw (under ideal conditions).

(2) The screw accelerated during the initial stage. When the speed increases to 800 r/min, the screw runs at a constant speed. Uniform deceleration movement is carried out before the end of the nut stroke. Lastly, the acceleration and deceleration values are all equal to 5 m/s^2.

(3) When the nut runs to the middle position of the lead screw stroke, it starts to deaccelerate uniformly. The nut's acceleration and deceleration value is equal to 5 m/s^2 during the entire movement.

The raceway wear depth of the nut in the course of 1 km under the above three working conditions is shown in Fig. 4. It can be seen that the raceway wear depth reaches the maximum value when the nut moves at variable speed throughout the entire running stroke. The raceway wear depth is minimal when the nut moves uniformly throughout the stroke. The main reason for this phenomenon is the unbalanced force and insufficient lubrication of the contact point between the ball and the raceway.

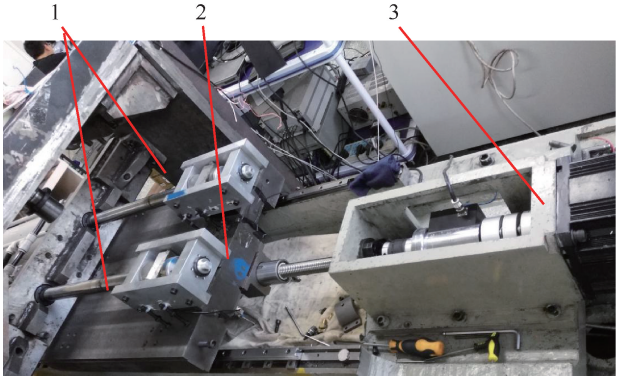

(a) Isoaxial side view of test

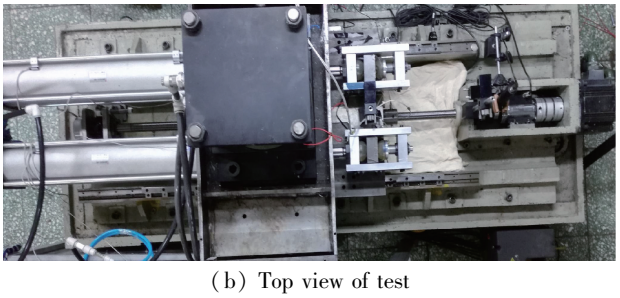

(b) Top view of test

1. cylinder; 2. the first nut; 3. driving motor

Fig. 3 Test for the computation of accelerated degradation of the ball-screw

4 Design of BSM's accelerated degradation test

A composite exponential accelerated degradation model [15-16] was established to analyze the accuracy degradation characteristics of the ball screw. The test samples are double-nut preloaded BSM, whose parameters are shown in Table 1. The initial preload value is 1500 N, the number of test samples is $n = 2$, and the number of acceleration test load levels is $h = 3$. The maximum load value applied in the test does not exceed 4500 N (three times the preload) to ensure that the precision degradation mechanism of BSM does not change. Moreover, the load value applied in the test is 2000 N, 3000 N, and 4000 N. According to the machining errors and installation and debugging differences of BSM, it can be concluded that the parameter variation of the ball screw is normally distributed $N(0.5\%)$. According to Ref. [15], the P-fractional precision life of the ball screw under normal working conditions is approximately equal to $\tau_p = 1.4246 \times 10^7 R$.

Table1 Parameters of the ball screw mechanism

Parameters	Value	Unit
(I) Geometry parameters of the ball screw		
Screw pitch cycle radius r	16	mm
Pitch L	10	mm
Contact angle β	40.2600	°
Helix angle α	5.6833	°
Screw inner radius of screw r_{CS}	16.182	mm
Nut inner radius of screw r_{CN}	15.818	mm
Radius of curvature of the screw raceway r_S	3.215	mm
Radius of curvature of the nut raceway r_N	3.215	mm
Ball's radius r_b	2.9765	mm
Preload F_{WS}	2562.8	N
Number of balls n_b	206	
Density of the ball material ρ	7.8	g/cm^3
Young's modulus E	211.1	GPa
Poisson's ratio v	0.3	
(II) The experimental conditions		
Room temperature	20	℃

Raceway wear degradation was calculated according to the compound exponential accelerated degradation model of BSM, as shown in Fig. 5. For the same ball screw load, raceway wear increases nonlinearly with an increase in revolutions. Similarly, raceway wear increases with load under the same number of revolutions. The simulated friction torque degradation curve that considers the error $\varepsilon \sim N(0, 0.05^2)$ distribution of the structural parameters of the ball screw is shown in Fig. 6.

Statistical analysis method and least square method were used to carry out data fitting of BSM simulation results for the accelerated stepping degradation, as shown in Fig. 7. Moreover, the accelerated degradation model of a compound exponential BSM was used for parameter estimation, and the estimated values of $\beta_{i,j}$ and α are shown in Table 2. The friction torque rapidly decreases in the initial and final stages of BSM precision degradation for the following reasons.

Table 2 The estimated value of parameter $\beta_{i,j}$ and α

Sample	$\beta_{i,j}$			α
	$S_1 = 2000$ N	$S_2 = 3000$ N	$S_3 = 4000$ N	
Sample 1	0.8786	1.0438	1.6313	1.0946
Sample 2	0.8546	1.0113	1.5506	1.0916

(1) There are burrs in the ball and the raceway in the early stage, which can be easily removed once the screw starts to run.

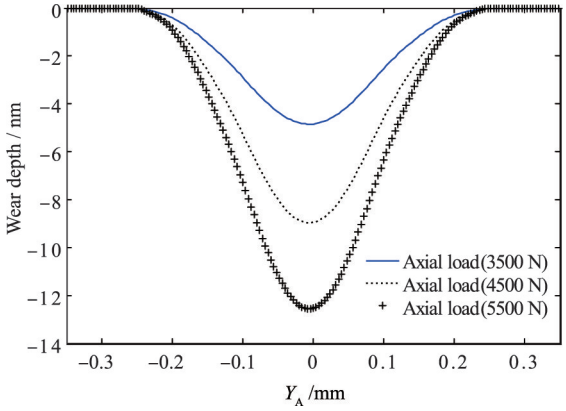

(a) Wear depth of nut raceway during uniform motion

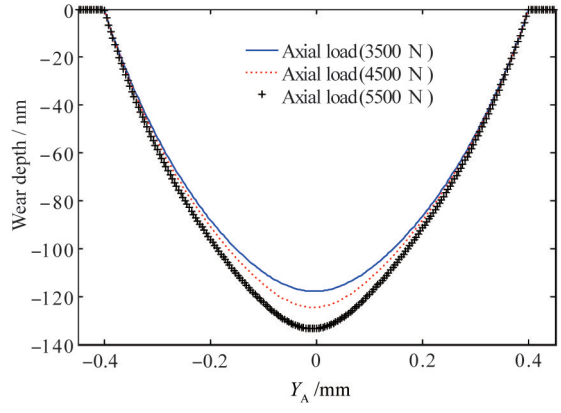

(b) Wear depth of nut raceway during mixed movement

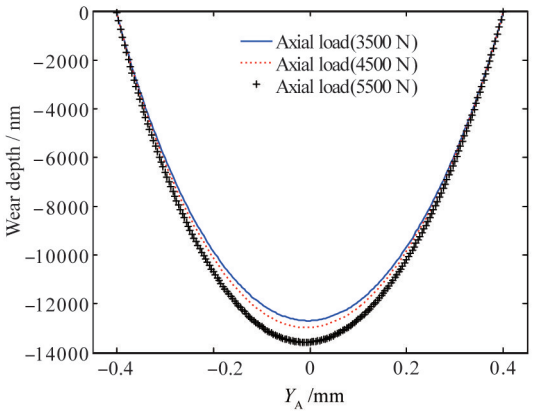

(c) Wear depth of nut raceway at uniform acceleration

Fig. 4 Distribution of the wear depth along the normal cross-section of the raceway under running motion state in the same stroke(1 km)

(2) The BSM preload degrades in the final stage, and the impact force of the ball movement in the raceway increases, aggravating the raceway wear.

Therefore, under the same operating conditions, the friction torque value of BSM in the initial stage, as opposed to the final stage, is greatly reduced.

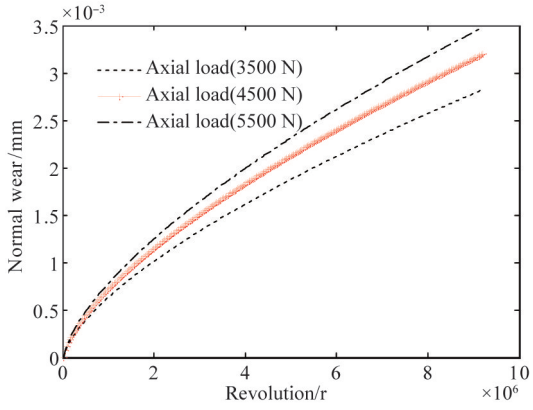

Fig. 5 The average degradation curve of raceway wear

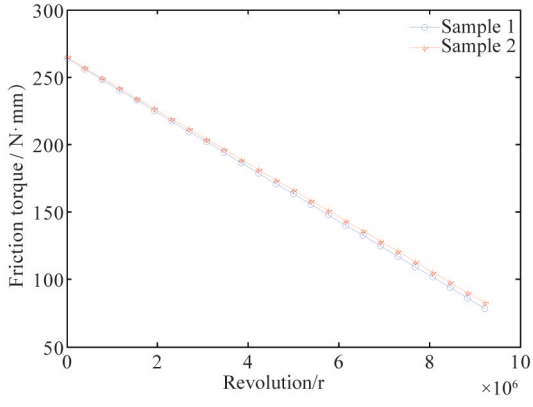

Fig. 6 Degradation simulation value of friction

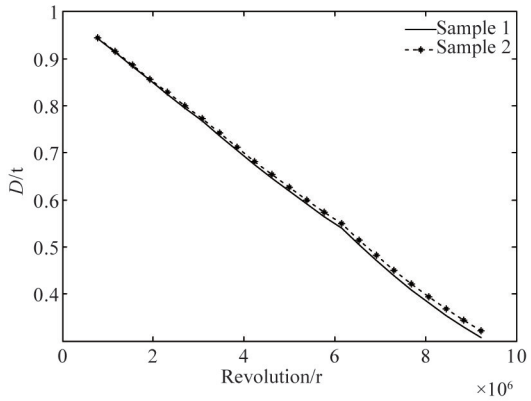

Fig. 7 Fitting results of the degradation curve of friction torque

According to the $\beta_i^{-1} \sim \text{Weibull}(\eta_i, m)$ model and $\beta_{i,j}$ value [15], the maximum likelihood estimation method is used to estimate parameters η_i and m_i, as shown in Table 3. BSM accelerated degradation model parameters b_{B0} and b_{B1} are calculated using the least square method according to the value of η_i and the formula $m_{k0} = \alpha m_B$, as shown in Table 4. According to the distribution parameter η_i and the stress function S_i, build a_i and function of load are shown in Fig. 8.

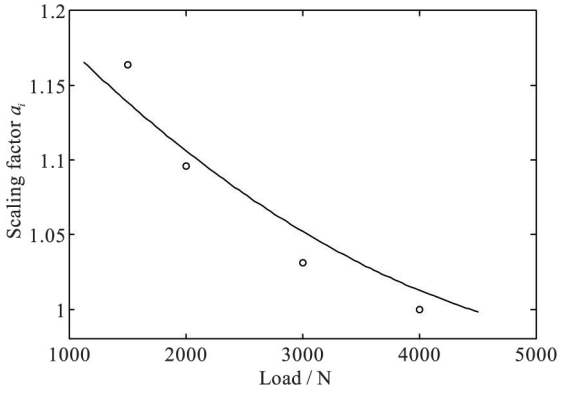

Fig. 8 The relationship between η_i and S_i

Table 3 The estimated value of parameter η_i and m_i

Parameter	$S_1 = 2000$ N	$S_2 = 3000$ N	$S_3 = 4000$ N	m_i
η_i	1.5535	1.48947	0.62570	3.52201

Table 4 The estimated value of parameter b_{B0} and b_{B1}

b_{B0}	b_{B1}
−1.2327	0.9294

5 Analysis of the accelerated degradation test results of BSM

The test adopts the timing truncation loading mode

to validate the BSM's compound exponential accelerated degradation model. The truncation (load holding) times for the three stages of the load level are $3.07 \times 10^6 R$, $3.07 \times 10^6 R$, and $3.07 \times 10^6 R$. The friction torque value was tested when the BSM ran at $2.9568 \times 10^5 R$ to accurately verify the accuracy degradation law of BSM. During the test, the chamber temperature was 15 – 40 ℃, oil lubrication model No. 32 was used, and the BSM test sample model was GD3210-P3. The acquisition process of the friction torque of the BSM is shown in Fig. 9. A constant screw rotation speed of 100 r/min was employed to accurately obtain the friction torque values of BSM at different stages of the precision degradation process. The variation curves of the friction torque at different stages are shown in Fig. 10. According to the analysis in Fig. 10, due to the existence of machining errors of ball screw, the friction torque value in the initial stage has a significant decline trend, but its change trend cannot truly reflect the accuracy degradation characteristics of ball screw. In the middle stage, the friction torque value of ball screw tends to decline gently and presents nonlinear changes. In the later stage, due to the wear of the ball screw, this causes the downward trend of the friction torque value of the ball screw to fluctuate greatly.

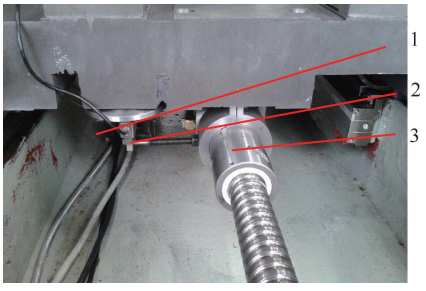

1. tension sensor; 2. moment arm; 3. the nut of ball screw

Fig. 9 Friction torque test diagram of BSM

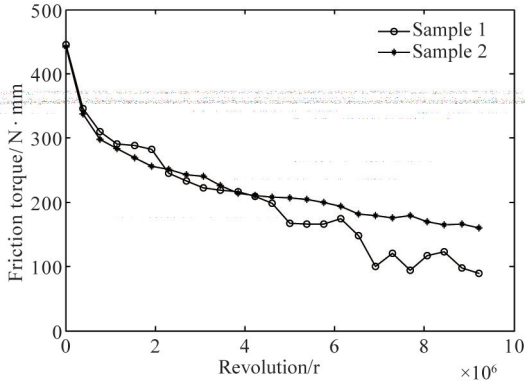

Fig. 10 The degradation curve of friction torque

The precision degradation model of BSM [16] was used to fit the friction torque value according to the statistical analysis method of stepping accelerated degradation test data of BSM. The obtained degradation law of BSM friction torque is shown in Fig. 11. It can be observed that the friction torque degradation curve of BSM can be used to accurately estimate its accuracy degradation characteristics, which is consistent with the predicted value of the simulation model.

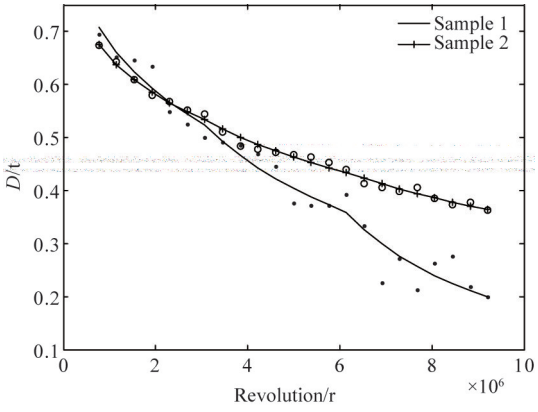

Fig. 11 Fitting results of the degradation curve of friction torque

The least square method was used to estimate $\beta_{i,j}$ and α parameters in the degradation model shown in Fig. 11. The estimated values are shown in Table 5.

Table 5 The estimated value of parameter $\beta_{i,j}$ and α

Sample	$\beta_{i,j}$			α
	$S_1 = 2000$ N	$S_2 = 3000$ N	$S_3 = 4000$ N	
Sample 1	1.0610	1.3752	2.1608	0.4514
Sample 2	0.9125	0.9979	1.1034	0.3397

The maximum likelihood estimation method is used to estimate parameters η_i and m according to the $\beta_i^{-1} \sim \text{Weibull}(\eta_i, m)$ model and $\beta_{i,j}$ value [15], as shown in Table 6.

Table 6 The estimated value of characteristic life

η_1	η_2	η_3	m
0.9465	1.1343	0.8561	3.0451

Moreover, the maximum likelihood estimation method is used to estimate parameters b_{B0} and b_{B1} according to the $\beta_i^{-1} \sim \text{Weibull}(\eta_i, m)$ model and η_i value [15], as shown in Table 7.

Table 7 The estimated value of parameters b_{B0} and b_{B1}

b_{B0}	b_{B1}
−0.1059	0.0412

A double-nut preloaded BSM was used as a sample in the accelerated degradation test. The allowable value was set to 5 μm to control the reverse nut difference within the allowable range. The maximum allowable degradation of the friction torque of the BSM can be set to approximately 30% of the initial value. Moreover, the BSM operates under the condition that the external load value does not exceed 2500 N. According to the BSM and friction torque test values, the BSM normally operates under a load value of $S_0 = 1500$ N. The friction moment degradation of the ball screw pair can be estimated according to Weibull distribution for $\eta_{Z,0} = 1.7742 \times 10^7 R$. The confidence interval of BSM samples is set to 90%, and the quantile as $P_{\text{fractile}} = 0.1$. Then, the P quantile time of BSM accuracy retention under normal operating conditions is obtained as $\tau_P = 1.341 \times 10^7 R$ revolutions. The BSM precision retention test life cycle error is 5.7% compared with the simulation value. Thus, the accuracy life cycle value of the BSM is acceptable according to the normal use of the ball screw. It can be concluded that the compound exponential accuracy degradation model of the ball screw pair selected in this paper can accurately reflect its accuracy degradation law.

6 Conclusions

In this paper, the BSM's compound exponential accelerated degradation model is established, and the model parameters are optimized. The maximum likelihood estimation method is used to estimate the accelerated degradation model parameters, ensuring the BSM accuracy under different stress levels and improving the accuracy of model parameters.

Firstly, the fractal wear analysis method is used to analyze the variation law of wear depth on the arc of the normal section of the BSM raceway under different operating conditions. The unbalanced force and insufficient lubrication of BSM under variable speed conditions are considered within the method. Moreover, the accelerated inertia load is accounted. Lastly, the lubrication failure and the boundary lubrication condition of uniform and variable speed are accounted.

An accelerated degradation test platform for ball screw accuracy retention is established. Three levels and two samples are used for the accelerated degradation test. The comparison between theoretical result and experimental result demonstrates that the friction moment of BSM is used as the evaluation index of ball screw accuracy degradation, providing a new research method for BSM accuracy retention investigations.

References

[1] SHIMODA H, TOSHA K, SHIMIZU S, et al. Rolling fatigue life and reliability of ball screws[C]// International Joint Tribology Conference. San Diego: ASME, 2007: 399-400.

[2] ZHANG Z Y, SONG X C, JIANG H K, et al. Study on exceptional wear of screw shaft groove in high-precision ball screw[J]. Tool Engineering, 2007, 42(1): 44-47. (In Chinese)

[3] FLEISCHER J, LEBERLE U, MAIER J, et al. Resource-efficient ball screw by adaptive lubrication[C]// The 21st CIRP Conference on Life Cycle Engineering. Trondheim: CIRP, 2014: 50-55.

[4] ZHEN N, AN Q. Analysis of stress and fatigue life of ball screw with considering the dimension errors of balls[J] International Journal of Mechanical Sciences, 2018, 137: 68-76.

[5] LI P, JIA X D, FENG J S, et al. Prognosability study of ball screw degradation using systematic methodology[J]. Mechanical Systems and Signal Processing, 2018, 109: 45-57.

[6] DENG Y F, DU S C, JIA S Y, et al. Prognostic study of ball screws by ensemble data-driven particle filters[J]. Journal of Manufacturing Systems, 2020, 56: 359-372.

[7] HUANG H F. Researches on performance degradation mechanism and its evaluation technology of NC machine tool ball screw pair[D]. Chengdu: Southwest Jiaotong University, 2013. (In Chinese)

[8] PENG C Y, TSENG S T. Progressive-stress accelerated degradation test for highly-reliable products[J]. IEEE Transactions on Reliability, 2010, 59(1): 30-37.

[9] SHEN J H. Study on Accuracy retention and test method of precision ball screw[D]. Nanjing: Nanjing University of Science and Technology, 2013. (In Chinese)

[10] CHENG Q, QI B B, LIU Z F, et al. An accuracy degradation analysis of ball screw mechanism considering time-varying motion and loading working conditions[J]. Mechanism and Machine Theory, 2019, 134: 1-23.

[11] ZHOU H X, ZHOU C G, FENG H T, et al. Theoretical and experimental analysis of the preload degradation of double-nut ball screws[J]. Precision Engineering, 2020, 65: 72-90.

[12] LIU J L, MA C, WANG S L. Precision loss modeling method of ball screw pair[J]. Mechanical Systems and Signal Processing, 2020, 135: 1-20.

[13] ZHAO J J, LIN M X, SONG X C, et al. Analysis of the precision sustainability of the preload double-nut ball screw with consideration of the raceway wear[J]. Proceedings of the Institution of Mechanical Engineers, Part J: Journal of Engineering Tribology, 2020, 234(9): 1530-1546.

[14] ZHANG L, GAO H L, DONG D W, et al. Wear calculation-based degradation analysis and modeling for remaining useful life prediction of ball screw[J]. Mathematical Problems in Engineering, 2018, 16: 1-18.

[15] WANG M, SUN R, ZHANG W, et al. Accelerated degradation test method for accuracy stability of precision ball screws[J]. Journal of Beijing University of Technology, 2016, 42(11): 1629-1633. (In Chinese)

[16] KONG D S, WANG M, SUN R, et al. Statistical analysis of

ball screw mechanism based on an accelerated degradation test[J]. Journal of Beijing University of Technology, 2017,43(11): 1629-1634. (In Chinese)
[17] KONG D S, WANG M, GAO X S. Effect of contact angle and helix angle on slide-roll ratio under the accelerated motion state of ball screw mechanism[J]. Journal of Southeast University (English Edition), 2017, 33 (4): 398-408.
[18] YAN W, KOMVOPOULOS K. Contact analysis of elastic-plastic fractal surfaces[J]. Journal of Applied Physics, 1998,84: 3617-3624.
[19] RABINOWICZ E. Friction and wear of materials[M]. 2nd edition. New York: Wiley, 1995: 14-43.
[20] WEN S Z, YANG P R. Elastohydrodynamic lubrication [M]. Beijing: Tsinghua University Press, 1992. (In Chinese)
[21] HU J Z, WANG M, GAO X S, et al. Axial contact stiffness analysis of position preloaded ball screw mechanism[J]. Journal of Mechanical Engineering, 2014, 50(7): 60-69. (In Chinese)

KONG Deshun, born in 1980. He received his Ph. D. degree in College of Mechanical Engineering and Applied Electronics Technology of Beijing University of Technology in 2017. He also received his B. S. degree in 2005 from Hebei Polytechnic University and M. S. degree from Shijiazhuang Railway Institute in 2009. His research interests include the design and calculation for key parts of CNC machine tools, analysis and control of vibration and noise of NC machine tools.